
CHAPTER IX

PHYLOGEOGRAPHY OF THE *RHABDITIS* (*PELLIODITIS*)

***MARINA* SPECIES COMPLEX: EVIDENCE FOR**

COSMOPOLITANISM, RESTRICTED GENE FLOW, RECENT

RANGE EXPANSIONS AND ACCELERATED EVOLUTION

In preparation:

Derycke S, Remerie T, Vierstraete A, Vanfleteren J, Vincx M, Moens T. Phylogeography of the *Rhabditis* (*Pellioditis*) *marina* species complex: evidence for cosmopolitanism, restricted gene flow, recent range expansions and accelerated evolution (in prep).

ABSTRACT

The nematode *Rhabditis (Pellioiditis) marina* has a worldwide distribution despite presumably low dispersal abilities. Recent studies on a local scale have illustrated that *R. (P.) marina* actually consists of several cryptic species which questions its true cosmopolitan distribution. We performed a phylogeographic study to identify micro- and macro-evolutionary processes shaping population structuring and speciation in the *R. (P.) marina* species complex. The mitochondrial COI gene was screened with the Single Strand Conformation Polymorphism method (SSCP) in 1292 specimens collected from decomposing macroalgae along the coasts of Western Europe, NE America, Mexico, South Africa and Australia. We found evidence for eleven cryptic species within *R. (P.) marina* that were sympatrically distributed. A strong genetic structuring was observed in all species and a genetic break was observed around the British Isles. A historical signature was present in species PmII showing evidence for two postglacial, northwards orientated expansions and for restricted gene flow with occasional long-distance dispersal. Our data also pointed to a contact zone in the Southern Bight of the North Sea. We found evidence for a true cosmopolitan distribution of nematode species due to occasional long-distance dispersal. In addition, an accelerated COI mutation rate was suggested for *R. (P.) marina*, which was about ten times higher than the generally applied molecular clock of 2 %. We further hypothesize that the cryptic radiation in *R. (P.) marina* is largely the result of allopatric speciation, and that the contemporary sympatric distribution results from occasional long-distance dispersal.

INTRODUCTION

The absence of obvious geographical barriers and the often large dispersal capacity of organisms in the marine environment have become a paradigm (e.g. Avise 1992, Dawson et al. 2001). Nevertheless, significant structuring of marine populations may be present (Barber et al. 2000, Rocha-Olivares et al. 2001, Perrin et al. 2004), even in species with pelagic larval stages (Taylor & Hellberg 2003). Explanations for marine speciation have concomitantly shifted from a focus on broad-scale allopatric speciation to mechanisms that may be situated at much finer geographical scales than anticipated (Taylor & Hellberg 2005). Biological characteristics (e.g. limited dispersal abilities, different habitat preferences), evolutionary processes (e.g. selection) and/or historical events may be responsible for differences in population genetic structuring and ultimately for the speciation of marine sister taxa (Palumbi 1994, Williams et al. 2001, Taylor & Hellberg 2005, Kelly et al. 2006).

Unraveling the effects of history, geography and biology requires a comparative approach between species differing in some aspects of their life-history. Such comparative studies have traditionally used distantly related species with a sympatric distribution (e.g. Avise 1992, Hellberg 1996, Bargelloni et al. 2005) or closely related sister taxa with different geographical distributions (Palumbi 1995, Sà-Pinto et al. 2005). Evidently, the large evolutionary and geographical differences between these species still fade the true pattern of genetic structure and speciation. In this way, cryptic radiations in the marine environment present an excellent opportunity to identify micro- and macro-evolutionary processes because they are likely to share a recent ancestor and are often sympatrically distributed (Dawson et al. 2002, Taylor & Hellberg 2005).

Cryptic species complexes are abundant in small invertebrates with a widespread distribution (Darling et al. 2004, Amato et al. in press, Gómez et al. 2007). Such transoceanic distribution is generally believed to be the result of either vicariance or dispersal events (Lessios et al. 1998). The discovery of cryptic radiations evidently questions the true cosmopolitanism of invertebrate species (Schroth et al. 2002, Le Gac et al. 2004) and corroborates the idea of very limited dispersal capacities. In contrast, evidence for long-distance dispersal has been documented in a saltwater rotifer (Suatoni et al. 2006) and in gastropods (Donald et al. 2005).

Marine nematodes are ubiquitously distributed around the world and typically outnumber other metazoan taxa in marine sediments in terms of density as well as diversity (Heip et al. 1985, Lambshhead & Boucher 2003). Although many nematode species contain spectacular morphological differentiations, their detection often requires high resolution microscopy (De Ley 2000). This is further illustrated in the recent discovery of substantial ‘cryptic’ diversity in two geographically widespread nematode species (Derycke et al. 2005, Derycke et al. 2007a). Phylogeographical studies in nematode species are rare and restricted to terrestrial, parasitic species (Plantard & Porte 2004, Nieberding et al. 2005). The free-living marine nematode *Rhabditis (Pellioiditis) marina* (Bastian 1865) inhabits decomposing macroalgae deposited in the intertidal zone of coasts and estuaries around the world, and may therefore disperse over considerable distances through rafting. A population genetic survey in *R. (P.) marina* showed restricted gene flow on a fairly small geographical scale (< 100 km, Derycke et al. 2005), suggesting that dispersal through rafting is rather limited. The genetic structuring at the local scale may have been confounded, however, by colonisation-extinction dynamics typical of ephemeral populations (Derycke et al. 2007b).

The present study aims to identify global patterns of genetic diversity in the *R. (P.) marina* species complex, which currently includes seven morphologically and genetically recognized species (see Chapter 7). Morphological distinction requires a suite of several morphometric characteristics. At least six species are sympatrically distributed in the Southern Bight of the North Sea (Derycke et al. 2006). In combination with low dispersal abilities and a worldwide distribution, the *R. (P.) marina* complex forms an excellent model to investigate patterns of micro- and macro- evolution. Based on the cryptic diversity and restricted gene flow patterns at a local scale, we expected to find 1) several new cryptic species, and 2) a strong genetic structure within each species.

As in terrestrial species, marine organisms may show genetic patterns consistent with northwards range expansions after retreatment of the ice (e.g. Wares & Cunningham 2001, Gysels et al. 2004). Therefore, we expected

to find a Pleistocene signature in the global contemporary genetic structure, with 1) the genetic pattern of a postglacial northward range expansion in the NE Atlantic populations, and 2) a reduced genetic diversity at higher latitudes. Because of their longterm isolation, we also expected to find 3) a clear genetic break between Atlantic and Mediterranean populations. At the same time, these results contribute to the understanding of the cosmopolitan distribution and dispersal abilities of marine nematodes, which are hitherto poorly studied.

MATERIAL AND METHODS

SAMPLING AND GENETIC ANALYSIS

From June 2005 until October 2006, *R. (P.) marina* were collected from numerous localities throughout Europe (6 Baltic, 12 Atlantic and 7 Mediterranean localities), NE America (3), Canada (1), Mexico (1), South Africa (1) and Australia (1) (Table 9.1). Specimens of *R. (P.) marina* were isolated from the same habitat type: decaying seaweeds and/or seagrasses washed ashore in the intertidal zone (except for the Baltic and Mediterranean locations, where tidal activity is limited). The organic material was incubated on marine agar dishes, allowing nematodes to move into the agar. This facilitated identification and sorting of living nematodes under a binocular: *R. (P.) marina* were handpicked from the agar and preserved on acetone until molecular processing. This resulted in 639 nematodes collected from 31 localities worldwide. We also added published genetic data on *R. (P.) marina* from a fine-scale population genetic survey in Belgium and the southwestern part of The Netherlands (Derycke et al. 2005, 2006). We took haplotype frequencies from Derycke et al. (2006) from localities with $n > 5$ and averaged them over seasons. Our total dataset thus comprised 1294 specimens from 42 localities (Table 9.1).

The mitochondrial cytochrome oxidase c subunit 1 (COI) gene was amplified according to Derycke et al. (2005). In short, DNA was extracted from single nematodes and 1 μ l was used for PCR with primers JB3 and JB5, yielding PCR-products of 426 bp long. These were screened for genetic variation with the Single Strand Conformation Polymorphism (SSCP) method. Distinct SSCP banding profiles were sequenced with the above primers on a ABI3130XL capillary DNA sequencer. Details on the sequencing procedure are described in Chapter 7. DNA samples were

stored at -80 °C so that different loci were amplified from the same individuals. We took a subset of samples containing representatives of each mitochondrial lineage and amplified two nuclear gene regions: the internal transcribed spacer region (ITS1-5.8S-ITS2) and the D2D3 region of the ribosomal LSU. Details on the amplification method can be found in Chapters 2 and 6. All new sequences will be deposited in GenBank.

DATA ANALYSIS

Phylogenetic analysis

COI sequences were aligned in ClustalX v 1.81 (Thompson et al. 1997) using default gap opening/extension costs of 15/6.66. Sequences of the closely related species *Rhabditis (Rhabditis) nidrosiensis* and of the congener *R. (P.) mediterranea* (Derycke et al. 2005) were added to the dataset. All 141 sequences were easily alignable and no indels were observed. Sequences were blasted in GenBank and translated in Mega v 3.0 (Kumar et al. 2004) to ensure sequence integrity.

Previous work on *R. (P.) marina* revealed high levels of regional genetic variation and the existence of a species complex (Derycke et al. 2005). To ensure that all sequences from our worldwide survey effectively belonged to this *R. (P.) marina* species complex, a neighbor-joining (NJ) tree using *P*-distances was constructed in Mega v 3.0 with trimmed COI sequences (396 bp). Three sequences (*n* = 2 for Florida, *n* = 1 for Mexico; haplotypes 18, 24 and 144 in Fig 9.1) were monophyletic and highly divergent with respect to all other rhabditid sequences (Fig 9.1). These misidentified nematodes were removed from the dataset. Mean sequence divergence within and between haplotype groups was calculated in Mega v 3.0 using the *P*-distance model.

The ITS alignment contained several indels and was screened for unreliable positions in SOAP 1.2a4 (Löytynoja & Milinkovitch 2001), which were removed for further phylogenetic analyses. The D2D3 contained no indels with respect to the *R. (P.) marina* complex and was aligned in ClustalX v1.81. For both nuclear fragments, a NJ tree was constructed using K2P-distances in Mega v 3.0.

The evolutionary model that best fitted the remaining mitochondrial and the nuclear sequences was determined with Modeltest 3.7 (Posada & Crandall 1998) using the Akaike Information Criterion (AIC). The HKY+I+G model best fitted the

COI data, GTR+I+G best fitted the D2D3 data, and GTR+G best fitted the ITS data. Most parsimonious (MP) trees were calculated using heuristic searches and a tree-bisection-reconnection branch swapping algorithm (10 000 rearrangements) with random stepwise addition of sequences in 100 replicate trials. Robustness of the trees was tested by bootstrapping with 1000 replications and 10 replicate trials of sequence addition. In addition, a Bayesian analysis was performed in MrBayes v 3.1.2 (Huelsenbeck & Ronquist 2005). MrModeltest 2.2 (Nylander 2004) identified the same evolutionary models as above. Four independent Markov chains were run for 500 000 generations, with a tree saved every 10th generation. The first 10 000 trees were discarded as burn-in.

Table 9.1: *Rhabditis (Pellioiditis) marina*. Listing of the waterbasin, country and location of the sampled populations. The total number of sampled specimens (n) along with the number of specimens belonging to each species are indicated. Haplotype diversity (h) and the standard error are also shown.

Waterbasin	Country	Location	Code	Latitude	Longitude	PmI		PmII		PmIIa		PmIIb		PmIV		PmV		PmVI		PmVII		PmVIII		PmIX		PmX		n
						n	h (SD)	n	h (SD)	n	h (SD)	n	h (SD)	n	h (SD)	n	h (SD)	n	h (SD)	n	h (SD)	n	h (SD)	n	h (SD)	n	h (SD)	
Pacific Ocean	Queensland	Cairns	Au	16°55' S	145°45' E							27	0.52 (0.03)														27	
NW Atlantic	Mexico	Yucatan	Me	21°12' N	87°48' W																			21	0.75 (0.06)		21	
NW Atlantic	USA	Florida	Fl	27°15' N	82°31' W					28	0.52 (0.03)																28	
Indian Ocean	South Africa	Transkei	Af	31°45' S	29°22' E												7	0.00 (0.00)							21	0.00 (0.00)	28	
Mediterranean	Greece	Crete	GrC	35°19' N	25°22' E												3	0.00 (0.00)			22	0.56 (0.10)					25	
NE Atlantic	Portugal	Tavira	Po	37°07' N	7°38' W											23	0.68 (0.08)										23	
Mediterranean	Spain	Alicante	Ali	38°40' N	0°07' E											2	-										2	
NE Pacific	Canada	Vancouver Island	Ca	39°35' N	125°50' W																						1	
NW Atlantic	USA	New York	NY	40°42' N	74°00' W					28	0.65 (0.05)																28	
Mediterranean	Spain	Palamos	Pa	41°50' N	3°07' E																29	0.58 (0.04)					29	
NW Atlantic	USA	Boston	Bo	42°21' N	71°03' W					30	0.56 (0.09)																30	
Mediterranean	Croatia	Mljet Islands	CrM	42°44' N	17°32' E																19	0.72 (0.08)					19	
Mediterranean	Greece	Lagonissi	GrL	42°44' N	25°53' E												22	0.80 (0.06)									22	
NE Atlantic	Spain	San Pedro	San	43°23' N	8°17' W									10	0.00 (0.00)												10	
Mediterranean	France	St Aygulf	Ay	43°23' N	6°43' E											11	0.76 (0.08)										11	
Mediterranean	Croatia	Brodarica	CrB	43°40' N	15°55' E																28	0.60 (0.06)					28	
NE Atlantic	France	Vaux sur mer	Va	45°38' N	1°04' W			3	-	16	0.00 (0.00)																19	
NE Atlantic	France	Sables d' Olonne	Sa	46°29' N	1°46' W					10	0.78 (0.09)							14	0.82 (0.06)								24	
English Channel	France	St Malo	Ma	48°38' N	2°01' W					39	0.75 (0.02)																39	
English Channel	France	Roscoff	Ro	48°43' N	3°59' W	1	-							1	-					21	0.83 (0.06)						23	
English Channel	Great Britain	Plymouth	Pl	50°22' N	4°9' E					31	0.74 (0.04)																31	
North Sea	Belgium	Nieuwpoort	Ni	51°09' N	2°43' E	44	0.84 (0.02)	2	-	16	0.43 (0.13)																62	
North Sea	Belgium	Blankenberge *	Bl	51°19' N	3°8' E	27	0.51 (0.11)	28	0.92 (0.03)	24	0.68 (0.04)						5	0.00 (0.00)							2	0.00 (0.00)	86	
North Sea	The Netherlands	Paulina *	Pa	51°21' N	3°49' E	43	0.87 (0.03)	17	0.83 (0.05)	12	0.62 (0.09)																72	
North Sea	The Netherlands	Kruispolderhaven *	Kr	51°22' N	4°3' E	48	0.67 (0.04)																				48	
North Sea	The Netherlands	Zeedorp *	Ze	51°24' N	3°58' E	43	0.78 (0.05)			32	0.74 (0.05)																75	
North Sea	The Netherlands	Breskens *	Br	51°24' N	3°33' E	49	0.68 (0.06)																				49	
North Sea	The Netherlands	Sloehaven *	Sl	51°27' N	3°36' E	41	0.79 (0.04)	17	0.23 (0.13)	36	0.70 (0.05)																94	
North Sea	The Netherlands	Oosterschelde *	Os	51°36' N	3°50' E	46	0.63 (0.07)			17	0.68 (0.06)																63	
North Sea	The Netherlands	Lake Grevelingen-Brouwershaven *	GrB	51°44' N	3°57' E			24	0.87 (0.05)	15	0.56 (0.01)			33	0.62 (0.06)												72	
NE Atlantic	Ireland	Cork	Co	51°53' N	8°23' W									5	0.80 (0.16)				2	0.00 (0.00)							7	
North Sea	The Netherlands	Lake Grevelingen-Scharendijke	GrS	51°54' N	3°49' E									29	0.64 (0.07)												29	
NE Atlantic	Great Britain	Wales	Wa	53°24' N	4°19' W			11	0.00 (0.00)																		11	
Baltic Sea	Germany	Kiel	Ki	54°19' N	10°08' E			1	-							1	-										2	
Baltic Sea	Poland	Isle of Rugia	Ru	54°30' N	13°24' E			9	0.22 (0.17)																		9	
Baltic Sea	Poland	Hel	He	54°36' N	18°48' E			4	-							10	0.69 (0.10)										14	
Baltic Sea	Poland	Kuznica	Ku	54°43' N	18°35' E			19	0.49 (0.10)																		19	
Baltic Sea	Germany	Flensburg	Fl	54°46' N	9°26' E			21	0.65 (0.07)																		21	
Baltic Sea	Germany	Sylt	Sy	55°01' N	8°26' E			9	0.42 (0.19)							10	0.71 (0.12)										19	
North Sea	North Scotland	Westroy	Sc	59°17' N	2°57' W	10	0.47 (0.13)									15	0.69 (0.07)										25	
North Sea	Norway	Aurlandsvangen	No	60°54' N	7°10' E			29	0.42 (0.11)																		29	
Atlantic	Iceland	Prestbakki	Ic	65°19' N	21°13' W	20	0.50 (0.12)							1	-												21	
TOTAL						372		289		254		27		79		79		29		23		98		21		23	1295	

* averaged across seasons (data from Derycke et al. 2006)

Phylogeographic and genetic structure analyses

A haplotype network was constructed using the minimum spanning network method in Arlequin v 2.0 (Schneider et al. 2000), and the statistical parsimony procedure in the program TCS v1.13 (Clement et al. 2000). Haplotypes were connected at the 95 % confidence level and ambiguities in the network were resolved according to the predictions of Crandall & Templeton (1993).

Based on concordance among phylogenetic trees and on previously reported genetic and morphological differentiation in *R. (P.) marina* (Derycke et al. 2005, Chapters 5 and 6), the mitochondrial sequence data were divided such that all sequences forming a monophyletic lineage were treated as species (see results). For each of these species, haplotype (h) and nucleotide (π) diversity and their standard deviation were calculated for each locality with Arlequin 2.0 (Schneider et al. 2000).

Patterns of genetic structuring among geographical localities ($n > 5$) for each species were estimated using Analysis of Molecular Variance (AMOVA). Significance levels were determined with 1000 permutations. Pairwise Φ_{ST} values among localities (and among regions) were calculated using Tamura & Nei distances (Tamura & Nei 1993). Due to low sample sizes and/or geographical restriction to one locality, AMOVA was not performed for the species PmVI, PmVII, PmIX and PmX²⁵. For the other six species, additional geographical structuring was investigated with a spatial analysis of molecular variance using SAMOVA 1.0 (Dupanloup et al. 2002). This procedure defines groups of populations that are geographically homogeneous and maximally differentiated from each other. In addition, pairwise Φ_{ST} values were calculated among populations.

The underlying patterns responsible for the genetic substructuring were investigated with a Nested Clade Analysis (NCA) using the program GeoDis 2.5 (Posada et al. 2000) on the parsimony network obtained with TCS. The NCA procedure assesses geographic association between haplotypes and uses the information embedded in the haplotype network to discriminate between historical events (e.g. fragmentation, expansion) and contemporary processes (e.g. gene flow)

²⁵ In Chapter 6, we found that lineages Z, Z2, Z3 and Z4 are cryptic species within the *R. (P.) marina* complex. We here renamed them according to the other cryptic species within the complex: Z = PmVI; Z2 = PmX; Z4 = PmIX. Because we currently have very limited information on Z3 (see Chapters 3 and 6), we do not discuss it further in this chapter.

responsible for the observed pattern of genetic variation (Templeton et al. 1995). The nesting design was constructed by hand on the parsimony network following the rules given in Templeton et al. (1987) and Templeton & Sing (1993). The statistical significance of the NCA distance measures was calculated by comparison with a null distribution derived from 1000 random permutations of clades against sampling localities. The NCA was restricted to PmII because it was the only species with an adequate sample design (i.e. geographical distribution and sample size).

Demographic analyses

The frequency distribution of pairwise sequence differences for each species was analysed by mismatch analysis and compared to the expected distribution under a sudden expansion model using 100 bootstrap replicates and quantifying the sum of squared deviations between observed and expected distributions (Rogers & Harpending 1992). The associated parameters (τ , θ_0 , θ_1) were also calculated. In addition, Tajima's D (Tajima 1989) and Fu's F_s (Fu 1997) neutrality test were performed to infer whether sequence evolution in the species was neutral. Significant negative values of both statistical tests indicate that the species has recently expanded. When all tests indicated a population expansion, the corresponding τ value was used to infer the mutation rate of COI (Pinceel et al. 2005) using the equation $\tau = 2 u t$, where u is the mutation rate of COI and t the time since expansion (Rogers & Harpending 1992). For this, we assumed that the expansion occurred during the interglacial periods (Weichselian, Eemian or Saalian), i.e. 14, 130 or 240 ky BP.

RESULTS

PHYLOGENETIC ANALYSIS

The screening of the COI gene in 640 specimens collected from around the world yielded 94 haplotypes, 83 of which not previously reported. The complete dataset (i.e. including Belgian and Dutch samples from Derycke et al. 2006) yielded a total of 1295 screened specimens and 136 haplotypes. The 396 bp long fragment contained 131 (33.1 %) variable sites, 103 of which were parsimony informative. Not all substitutions were synonymous, and the amino acid alignment yielded 11 polymorphic sites (8.3 % variable sites), one of which was fixed in two species (PmI and PmIV) and nearly fixed in a third (PmIII).

Phylogenetic analyses of the mitochondrial and nuclear genes identified eleven highly supported lineages (PmI – PmX, PmIIIb), that were monophyletic with respect to *R. (R.) nidrosiensis* in the NJ analysis (Fig 9.1). The congener *R. (P.) mediterranea* was mixed among the *R. (P.) marina* species. The taxonomic status of the Z3 branch has been discussed in Chapter 6 and because of the limited number of specimens and data on this branch, we do not treat it further here. The mitochondrial lineages PmVI and PmIX collapsed into a single well supported clade in the nuclear gene trees. This pattern was also observed for PmVII and PmVIII. Nevertheless, we treat these four mitochondrial lineages as species based on their allopatric distribution (see next section). In addition, morphological differences between PmVI and PmIX have been documented (see chapter 6). A substructuring within the mitochondrial clades PmIII (subclades a and b) and PmV (subclades a, b and c) was present (Fig 9.1A). For PmV, this structuring could not be attributed to geography and it was absent in the nuclear genes (Fig 9.1B and C). We therefore treated the three subclades as intraspecific variation of PmV. Subclade b of PmIII was highly supported in the nuclear genes, and was found allopatrically from subclade a. PmIIIb was thus also treated as a species. The single individual from Canada did not belong to any of these eleven species. Haplotypes within each species were very similar (divergence 1.0 - 2.6 %), while haplotypes from different species were separated by at least 17 substitutions (divergence 4.4 – 12.7 %, Table 9.2).

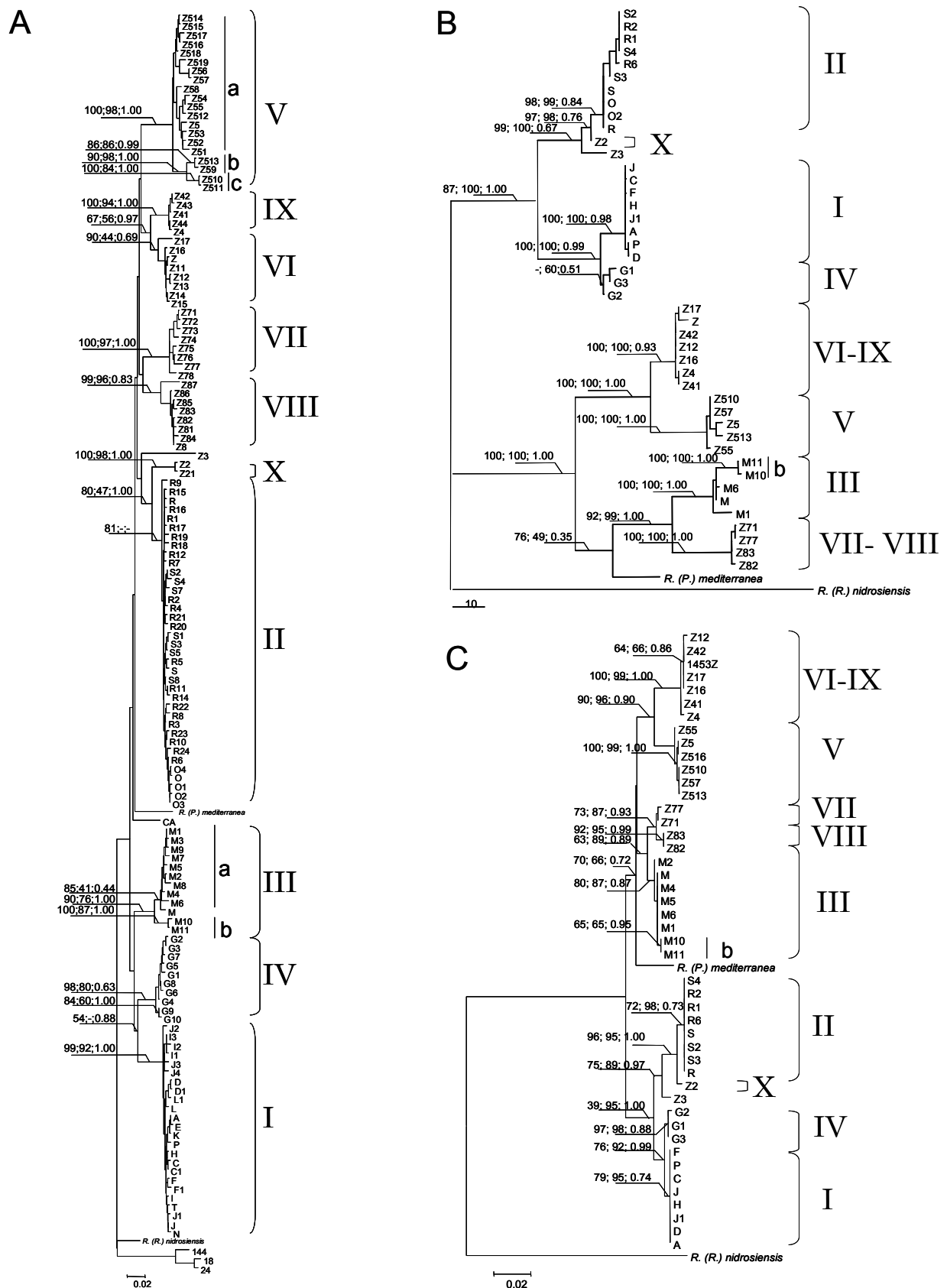


Fig. 9.1: *Rhabditis (Pellioiditis) marina*. A. Neighbor-joining (NJ) tree of COI based on P-distances. B. NJ tree of the ITS region based on K2P distance. C. NJ tree of the D2D3 region based on K2P distances. Values above branches are bootstrap values for MP, NJ and Bayesian probabilities. Cryptic species are designated with roman numerals.

	PmI	PmII	PmIIIa	PmIIIb	PmIV	PmV	PmVI	PmVII	PmVIII	PmIX	PmX	Z3	Ca	<i>R. (P.) med</i>	<i>R. (R.) nidro</i>
PmI	1.0 ± 0.2														
PmII	8.8 ± 1.4	1.0 ± 0.2													
PmIIIa	7.8 ± 1.3	8.8 ± 1.4	1.0 ± 0.2												
PmIIIb	8.2 ± 1.3	9.1 ± 1.3	3.3 ± 0.8	0.5 ± 0.3											
PmIV	6.6 ± 1.1	7.9 ± 1.3	7.0 ± 1.2	7.2 ± 1.2	1.0 ± 0.3										
PmV	9.9 ± 1.4	9.1 ± 1.3	8.7 ± 1.3	9.4 ± 1.3	9.0 ± 1.3	2.6 ± 0.5									
PmVI	10.1 ± 1.5	7.0 ± 1.2	7.2 ± 1.2	7.8 ± 1.2	8.1 ± 1.3	8.5 ± 1.3	1.2 ± 0.3								
PmVII	9.8 ± 1.4	8.3 ± 1.2	8.7 ± 1.3	9.2 ± 1.4	10.7 ± 1.5	9.8 ± 1.4	7.4 ± 1.2	1.5 ± 0.4							
PmVIII	9.7 ± 1.5	7.8 ± 1.3	7.4 ± 1.2	7.4 ± 1.2	9.1 ± 1.4	9.7 ± 1.4	7.9 ± 1.3	8.1 ± 1.3	1.4 ± 0.3						
PmIX	9.6 ± 1.4	7.4 ± 1.2	7.6 ± 1.2	7.3 ± 1.2	9.3 ± 1.4	8.4 ± 1.2	4.4 ± 0.9	8.0 ± 1.2	7.9 ± 1.2	0.5 ± 0.2					
PmX	10.2 ± 1.6	4.7 ± 1.0	9.1 ± 1.4	8.8 ± 1.3	9.0 ± 1.4	9.5 ± 1.4	7.7 ± 1.3	8.0 ± 1.3	9.3 ± 1.4	7.8 ± 1.3	0.5 ± 0.3				
Z3	11.4 ± 1.5	9.0 ± 1.4	11.2 ± 1.5	12.0 ± 1.6	11.0 ± 1.5	11.6 ± 1.5	10.1 ± 1.5	10.7 ± 1.5	11.4 ± 1.6	11.3 ± 1.5	10.6 ± 1.6	-			
Ca	9.2 ± 1.5	7.0 ± 1.2	6.7 ± 1.2	6.6 ± 1.2	8.2 ± 1.3	9.4 ± 1.4	7.7 ± 1.3	8.0 ± 1.3	8.3 ± 1.3	8.3 ± 1.4	7.7 ± 1.3	9.7 ± 1.5	-		
<i>R. (P.) med</i>	10.5 ± 1.4	8.0 ± 1.3	8.0 ± 1.3	8.6 ± 1.4	9.3 ± 1.4	9.8 ± 1.4	6.7 ± 1.2	10.0 ± 1.4	9.6 ± 1.4	8.8 ± 1.4	8.6 ± 1.4	11.7 ± 1.6	7.6 ± 1.4	-	
<i>R. (R.) nidro</i>	7.8 ± 1.3	8.3 ± 1.3	8.0 ± 1.3	8.3 ± 1.3	8.5 ± 1.3	10.7 ± 1.4	9.2 ± 1.4	9.9 ± 1.4	9.6 ± 1.4	8.0 ± 1.3	9.3 ± 1.4	12.7 ± 1.7	8.1 ± 1.4	9.1 ± 1.4	-

Table 9.2 Sequence divergences within and between species of the *R. (P.) marina* complex. Mean within-group sequence divergence ± standard error (diagonal) and mean between-group divergences ± standard error are based on the P-distances. Sequences Z3, *R. (P.) mediterranea* (*R. (P.) med*) and *R. (R.) nidrosiensis* (*R. (R.) nidro*) are from Derycke et al. (2005) and Chapter 6.

PHYLOGEOGRAPHY OF THE *R. (P.) MARINA* SPECIES COMPLEX

The species showed a dominant pattern of sympatry in the Atlantic samples, while Mediterranean samples mostly contained one species (Fig. 9.2). Three species were highly abundant: PmI was almost exclusively present in the North Sea, while PmII showed a continuous range from the Bay of Biscay to the Baltic Sea. PmIII was less abundant in this range, but it was the dominant species along the east coast of North America, yielding a transatlantic distribution range (Fig. 9.2). PmIIIb was found in Australia. PmIV was also widespread along the European Atlantic, with the exception of the Baltic region. None of these five species were encountered in the Mediterranean samples, which were dominated by PmV and PmVIII. The latter species was restricted to the Mediterranean Sea. PmV on the other hand had a very discontinuous distribution range: in addition to the Mediterranean, it was encountered in Po, Sy and in the Baltic samples, but was absent in any intermediate Atlantic locality. The remaining four species (PmVI, PmVII, PmIX, PmX) were only sampled at low frequencies (Fig. 9.2). PmVI was found in the North Sea, Bay of Biscay, Mediterranean and South Africa. PmVII was restricted to the English Channel and PmIX to Mexico. Finally, PmX was found in the North Sea and South Africa.

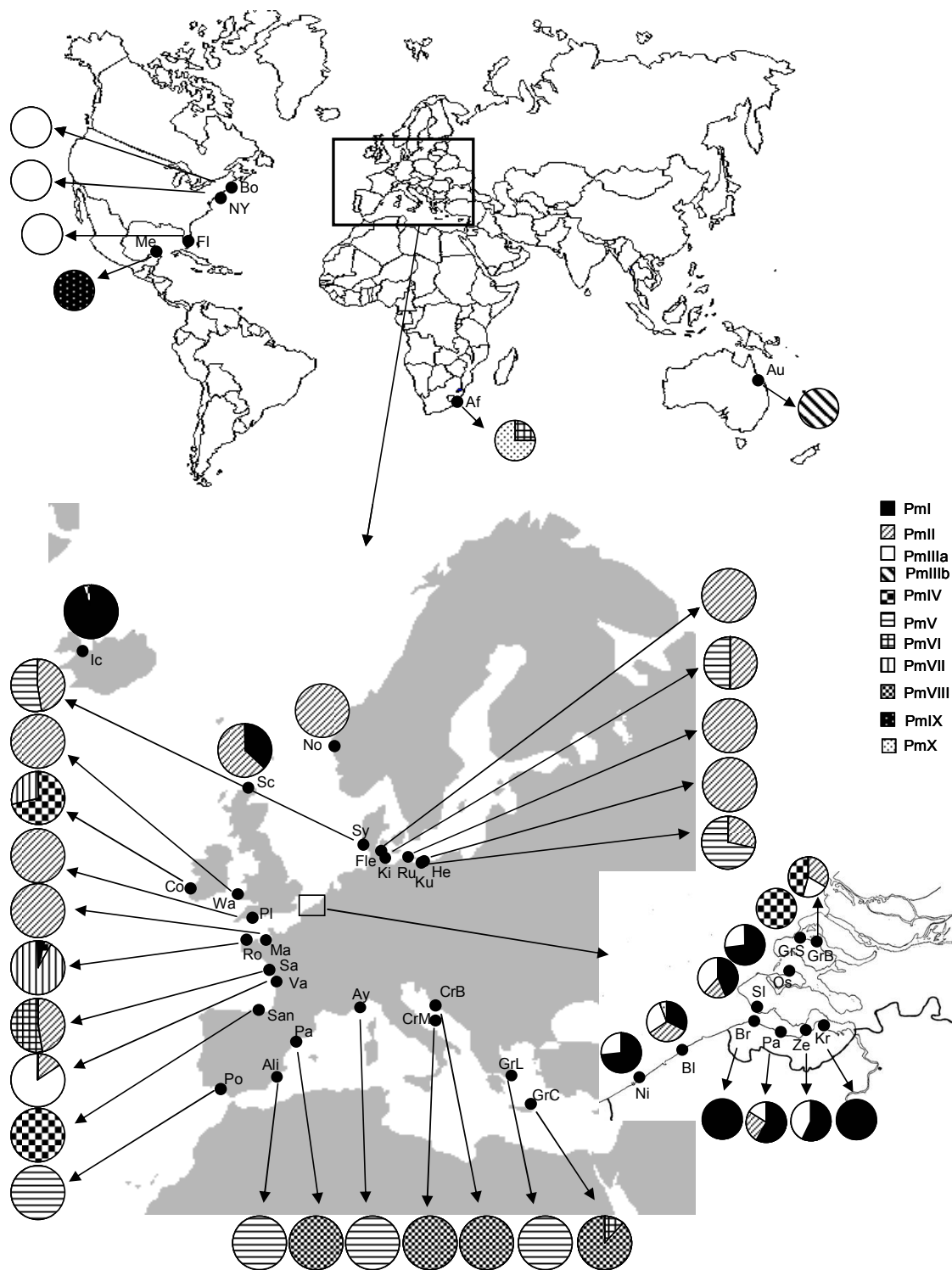


Fig. 9.2 *Rhabditis (Pellioiditis) marina*. Distribution of the eleven cryptic species in the sampled localities. Abbreviations of localities are as in Table 9.1

SPATIAL GENETIC STRUCTURING WITHIN THE CRYPTIC SPECIES

Pairwise Φ_{ST} values for each species are summarized in Appendix 9.1. AMOVA indicated the presence of a significant genetic structuring in PmI, PmII, PmIIIa, PmIV, PmV and PmVIII (Table 9.3), and SAMOVA detected an additional geographical structuring in PmI and PmII. For PmI, 43.85 % of the genetic variation was significantly attributed to a grouping of Iceland/North Scotland and the Belgian/Dutch samples. For PmII, one location from the Westerschelde (Sl) and samples from the NE North Sea (Sy) and Baltic Sea (Fl, Ku, Ru) were highly differentiated from each other and from all other samples (Appendix 9.1). Nevertheless, a grouping of No, Sc, Wa, Sy, Fle, Ku, Ru into a northern group and of Sl, Bl, Gr, Pa, Pl, Ma, Sa into a southern group explained an additional 19.3 % of the observed genetic variation in PmII ($p < 0.001$).

	n	%	Φ_{st}	p
PmI	370			
Among populations		22.35	0.22	***
Within populations		77.65		
PmII	281			
Among populations		36.91	0.37	***
Within populations		63.09		
PmIII	281			
Among populations		62.54	0.63	***
Within populations		37.46		
PmIV	77			
Among populations		60.29	0.60	***
Within populations		39.71		
PmV	76			
Among populations		39.31	0.39	***
Within populations		60.69		
PmVIII	98			
Among populations		27.56	0.27	***
Within populations		72.44		

Table 9.3 *Rhabditis (Pellioiditis) marina*. AMOVA results for the species occurring in several locations and with $n > 5$. The number of individuals in the analysis (n), the amount of variation explained by differences among and within populations (%), the Φ statistics and the significance level (p) are shown. *** $p < 0.001$.

The highest amount of variation was observed between populations of PmIV and the lowest between populations of PmIIIa (60 % and 20 %, respectively, Table 9.3). Given the transoceanic distribution of PmIII, this low genetic differentiation was surprising. Pairwise Φ_{ST} values between PmIIIa populations on both sides of the Atlantic generally were low and non-significant

(Appendix 9.1). The structuring was mainly caused by the Bay of Biscay location (Va), which was in most cases differentiated from the locations in Belgium and The Netherlands. Similarly, a strong genetic differentiation was observed for PmIV between the Bay of Biscay (San) and all other locations. The single haplotype that was encountered in Iceland was more closely related to the haplotypes from The Netherlands and Cork than it was to the Biscay haplotypes, while the opposite was true for the Roscoff haplotype (Fig. 9.3).

For PmV, the northern samples Sy and He were not significantly differentiated from each other, while the southern populations (Po, GrL, and Ay) were (Appendix 9.1). Interestingly, the Po sample was not significantly differentiated from the northern Sy sample, and the Baltic sample (He) not from the Mediterranean Ay sample. Finally, low but significant Φ_{ST} values were noticed between all four Mediterranean populations of PmVIII.

PHYLOGEOGRAPHY AND DEMOGRAPHIC HISTORY OF THE CRYPTIC SPECIES

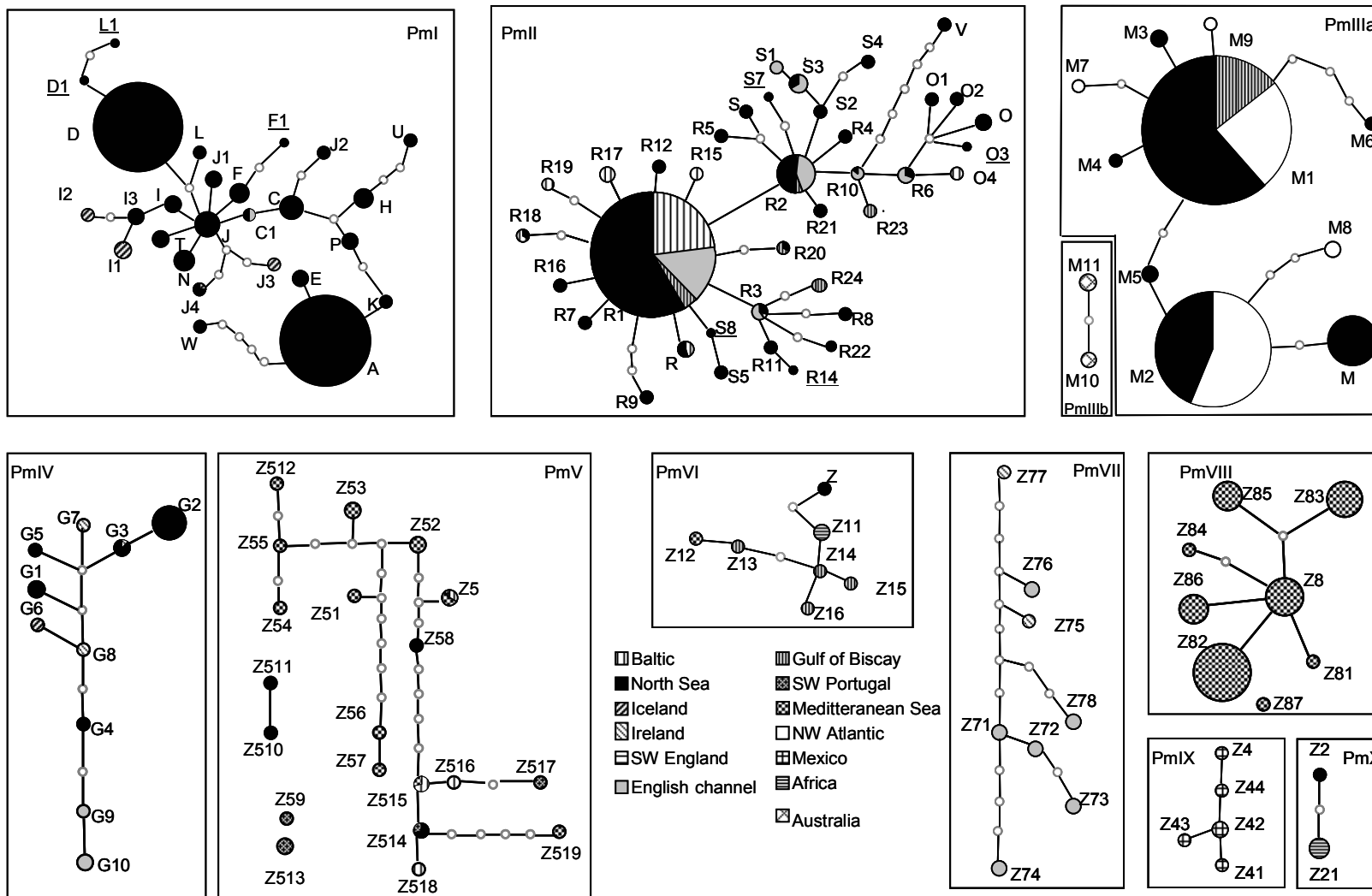
The maximum parsimony network yielded several unconnected haplotypes and/or haplotype groups corresponding to the different phylogenetic species (Fig. 9.3). Of all haplotypes, 57 were shared among sampling localities and 79 haplotypes were location specific. PmI and PmII, and to a lesser extent PmIIIa, PmVI and PmVIII, displayed a star shaped network (Fig. 9.3). The tip haplotypes of all networks were largely constrained to a particular geographic region, while central haplotypes of lineages PmII and PmIIIa were shared among populations throughout their distribution.

The goodness-of-fit test of the mismatch distributions showed that six out of the nine mitochondrial clades fitted a model of sudden expansion (Table 9.4), but Tajima's D and Fu's Fs were significantly different from zero and negative only for clade PmII. We used the mismatch distribution parameter τ accompanying the expansion of PmII to calculate the divergence rate of the COI gene, assuming that the approximate time of expansion occurred after one of the last three glacial periods. This yielded divergence rates of 21.7 %, 2.3 % and 1.3 % per MY, respectively.

	PmI	PmII	PmIIIa	PmIV	PmV	PmVI	PmVII	PmVIII	PmIX
Mismatch mean	2.84	2.5	1.78	3.43	9.8	1.86	5.12	1.81	1.14
θ_0	0.001	0.52	0.0	0.012	3.01	0	0.002	0	0
θ_1	14.62	8.8	3.16	4.37	24.1	470	21.12	19.9	1892
ζ	3.69	2.41	2.94	9.1	10.3	2.14	6.9	2.33	1.28
SSD (p)	0.04 ***	0.001 (ns)	0.08 (ns)	0.04 (ns)	0.01 (ns)	0.006 (ns)	0.05 (*)	0.04 (***)	0.007 (ns)
Raggedness(p)	0.09 ***	0.016 (ns)	0.32 (*)	0.08 (ns)	0.02 (*)	0.05 (ns)	0.08 (ns)	0.11 (*)	0.11 (ns)
Tajima's D (p)	-0.76 (ns)	-1.59 *	-0.006 (ns)	1.13 (ns)	1.43 (ns)	0.41 (ns)	0.92 (ns)	0.4 (ns)	0.08 (ns)
Fu's Fs (p)	-4.5 (ns)	-26.04 ***	1.91 (ns)	1.10 (ns)	1.1 (ns)	-1.22 (ns)	1.26 (ns)	0.82 (ns)	-0.71 (ns)

Table 9.4 *Rhabditis (Pellioditis) marina*. Mismatch distribution parameters and results of Tajima's and Fu's neutrality tests. The significance level is indicated between brackets. (ns) not significant, * $p < 0.05$, ** $p < 0.01$, *** $p < 0.001$.

Fig. 9.3 *Rhabditis (Pellioiditis) marina*. TCS network with 95 % confidence connection between haplotypes. Circles are proportional to haplotype abundances and are shaded according to geographical occurrence. Small empty circles are hypothetical mutations.



NESTED CLADE ANALYSIS OF PmII

The nesting procedure on the TCS network of the PmII haplotypes resulted in three clade levels (Fig. 9.4). NCA detected a significant association between genetic variability and geographic distribution for several clades at all clade levels (Table 9.5, Fig. 9.4). At the lowest nesting group, genetic variation was mainly the result of restricted gene flow with isolation by distance (clades 1-1, 1-14). This pattern was observed almost throughout the entire distribution range of PmII: the Bay of Biscay, English Channel, North Sea and Baltic Sea. In addition, a recent contiguous range expansion was detected from the Bay of Biscay through the English Channel in the northern part of the North Sea (clade 1-11). For clade 1-19, some evidence for IBD was found, but the pattern could not be distinguished from range expansion and fragmentation due to inadequate sampling.

At the higher nesting levels, restricted gene flow with isolation by distance remained the dominant underlying pattern for the observed genetic variation, although some evidence was present for occasional long distance dispersal between the Bay of Biscay and the northern part of the North Sea (clade 2-1). The 2-3 clade was found along the SW and N coasts of Great Britain, in Norway and in Sylt, and NCA detected a signal of range expansion along Great Britain (Fig. 9.5A). There was, however, insufficient genetic resolution to distinguish between range expansion and restricted gene flow.

The total cladogram consisted of three clades, the oldest being the interior 3-2 clade which was abundant from the southernmost location (Va) over the English Channel and the SW part of the North Sea. The younger 3-1 tip clade dominated the British Isles, the Baltic region and the North Sea. The 3-3 clade overlapped with the 3-1 and 3-2 clades in the English channel and the southern part of the North Sea (Fig. 9.5B). According to the NCA, the distribution of the three-level clades was caused by a range expansion.

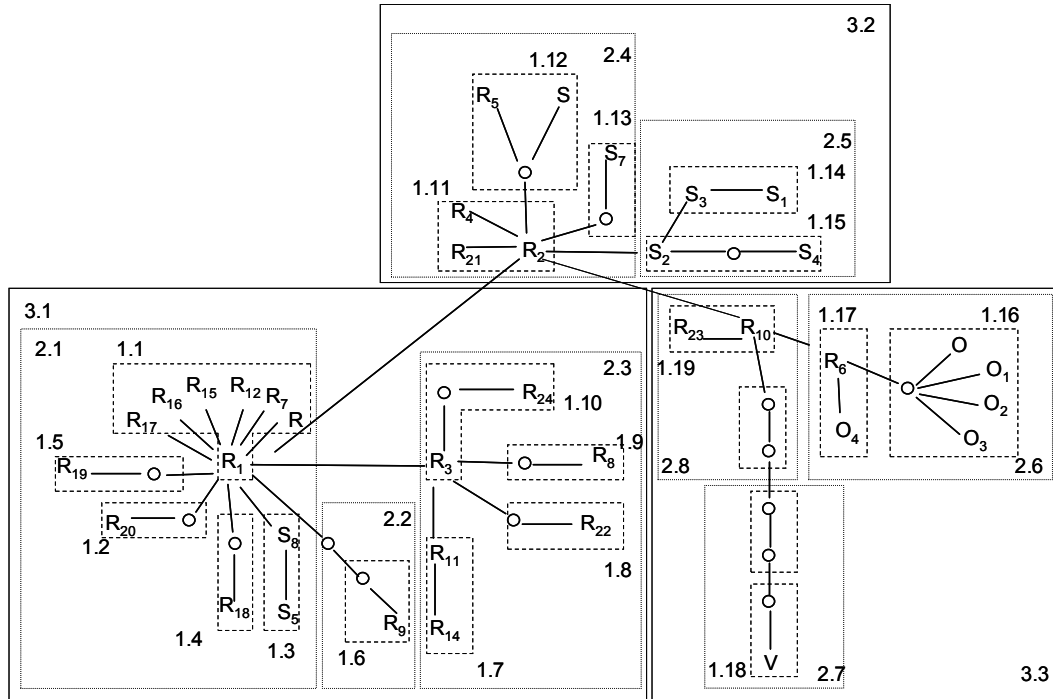


Fig. 9.4 *Rhabditis (Pellioditis) marina*. TCS network among the PmII haplotypes with indication of the nesting design used in the Nested Clade Analysis.

Clade	Chi-square	P	Inference	
1-1	336.9	< 0.0001	1-2-3-4-No	Restricted gene flow with isolation by distance
1-3	2.0	1.0		
1-7	5.0	0.21		
1-10 *	11.0	0.19		
1-11	42.0	< 0.0001	1-2-11-Yes-12-No	Contiguous range expansion
1-12	6.0	0.06		
1-14	20.0	< 0.0001	1-19-20-2-11-17-4-No	Restricted gene flow with isolation by distance
1-15	4.95	0.06		
1-16	55.0	< 0.0001		No interior tips
1-17	12.0	0.08		
1-19	11.0	0.002	1-2-3-5-15-16-18-No	Geographical sampling scheme inadequate to discriminate between fragmentation, range expansion, and isolation by distance
2-1	123.6	0.001	1-2-3-5-6-7-8-No	Sampling design inadequate to discriminate between isolation by distance (short distance movements) versus long distance dispersal
2-3*	72.0	< 0.0001	1-2-3-5-6- Too few clades	Insufficient genetic resolution to discriminate between range expansion/colonization and restricted dispersal/gene flow
2-3*	72.0	< 0.0001	1-2-3-5-6-Too few clades	Insufficient genetic resolution to discriminate between range expansion/colonization and restricted dispersal/gene flow
2-4	22.9	0.09		
2-5	27.4	< 0.0001	1-2-3-4-No	Restricted gene flow with isolation by distance
2-6	28.7	< 0.0001	1-2-19-20-2-3-4-No	Restricted gene flow with isolation by distance
3-1	72.9	0.01	1-2-3-4-No	Restricted gene flow with isolation by distance
3-2	7.71	0.36		
3-3	20.3	0.10		
Total	264.4	< 0.0001	1-2-11-Yes	Range expansion

Table 9.5 Inferences from the Nested Clade Analysis using the nesting design in Fig. 9.4 (see Templeton 1998 for details). * alternative connection possible, but with the same results.

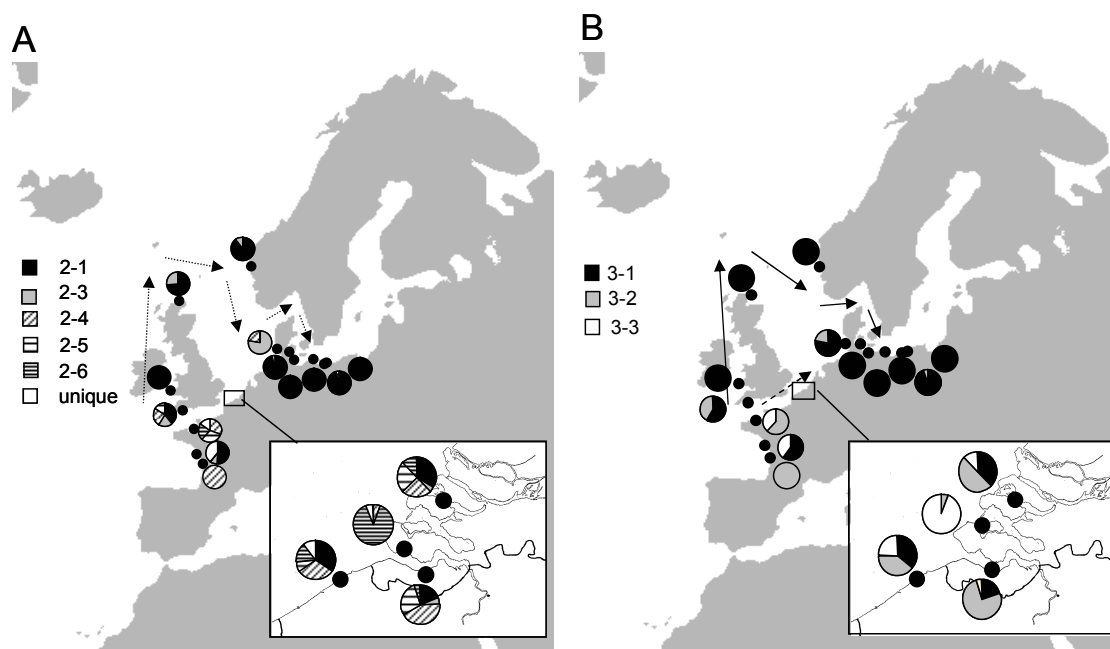


Fig 9.5: Geographical distribution of the 2- and 3-step clades of *PmII*. (A) Distribution of the 2-step clades with indication of the possible range expansion of clade 2-3. (B) Distribution of the 3-step clades with indication of their range expansions. The clades are the result of the NCA and are shown in Fig 9.4

HAPLOTYPE DIVERSITY IN *PMII*

The haplotype diversity of *PmII* shows a slight decreasing trend with latitude (Fig. 9.6). The higher h was observed in the southernmost populations and was slightly lower in the Baltic and northern North Sea populations (except in locations Fle and Sc). The diversity in the Southern Bight of the North Sea and the Brittany populations is, however, not significant lower than in the southern populations.

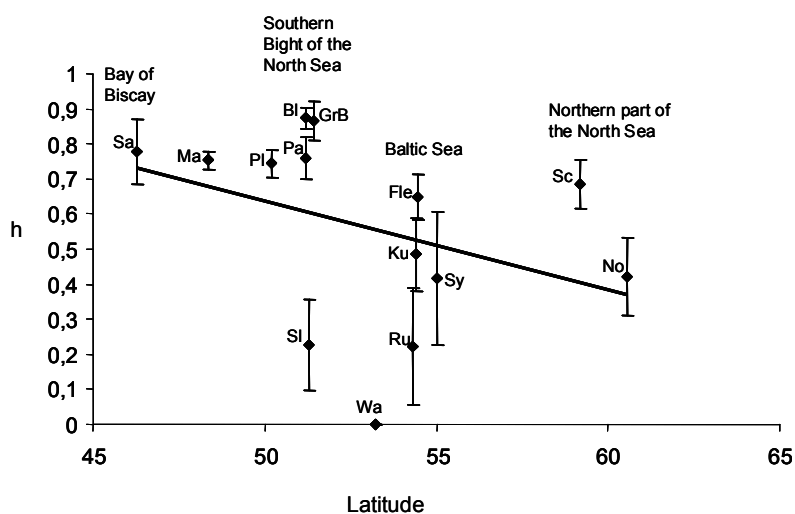


Fig. 9.6 *Rhabditis (Pellioiditis) marina*. Haplotype diversity (h) of *PmII* across latitude. Error bars are standard deviations. Geographical regions are indicated, sample abbreviations are as in Table 9.1.

DISCUSSION

R. (P.) marina is composed of at least 11 genetically highly divergent lineages, seven of which have previously been designated as ‘cryptic’ species based on molecular and morphological data (Chapters 5 and 6). Lineages PmIIIb, PmV, PmVII and PmVIII are new in this study. Based on concordance patterns between mitochondrial and nuclear gene trees and geographical distribution, these four new lineages were considered additional cryptic species within the *R. (P.) marina* complex. Morphological data are required to confirm this hypothesis.

MICR- EVOLUTIONARY PROCESSES AFFECTING POPULATION GENETIC STRUCTURE

Gene flow and migration

Based on the genetic patterns on a local scale (Derycke et al. 2006, 2007a), we expected deep levels of population structure in all species of the *R. (P.) marina* complex on a global scale. Indeed, a highly significant structuring was observed in all cryptic species of sufficient sample size, indicating that gene flow is limited between populations within the *R. (P.) marina* complex. Based on the Φ_{st} values, we infer two general patterns of dispersal. Significantly high pairwise Φ_{st} values were observed between populations from different biogeographical areas (e.g. between the northern part and the Southern Bight of the North Sea for PmI, between the Baltic and the North Sea locations for PmII) while non-significant values were observed between geographically proximate populations (e.g. in the Westerschelde estuary). There were, however, some exceptions to this general pattern. For example, no differentiation was observed between some NE and NW Atlantic populations of PmIIIa and between Baltic and Mediterranean populations of PmV. In addition, the transcontinental distribution of PmIII, PmVI and PmX suggests that effective long-distance dispersal has occurred in at least some species of the *R. (P.) marina* complex. In the case of PmIII, the presence of two haplotypes (M1, M2) at relatively high abundances on both sides of the Atlantic may be explained by multiple colonisation events or by a large dispersal propagule (Wares & Cunningham 2001). In view of its life-history characteristics, *R. (P.) marina* could indeed disperse over considerable distances by rafting on macroalgae, which may be the only possible means of dispersal over large stretches of ocean for marine intertidal species with direct development. The

importance of rafting in the marine environment has been recognized (Thiel & Gutow 2005, Vandendriessche et al. 2006) and rafting has been proposed for several intertidal marine invertebrates lacking long-lived larvae (Ó Foighil et al. 1999, Thiel & Gutow 2005, Donald et al. 2005). The NCA results in PmII showed, however, that long-distance dispersal only occurs sporadically. This is further strengthened by the presence of unique haplotypes in the distant populations of PmIII, PmVI and PmX, and by the lack of a transcontinental distribution in the other lineages. Therefore, a large dispersal propagule with many haplotypes may be the best explanation for the transatlantic pattern in PmIII. In view of the present watercurrents between Europe and America, this dispersal event probably occurred when both continents were connected via watercurrents. Alternatively, dispersal may have been mediated through the transport of ship ballast water or through migrating birds on a contemporary timescale.

Additional geographical structure was observed in PmI and PmII, in which northern populations of the North Sea and/or Baltic Sea were genetically more similar to each other than to the southern populations of the English Channel and Bay of Biscay. This genetic break coincided around the British Isles in all Atlantic species, suggesting that the genetic structure in the *R. (P.) marina* species was influenced by historical events.

Historical events

The dramatic climate changes of the last few million years, with extensive oscillations during the last 700 ky, are probably one of the most important historical events influencing the distribution of many temperate species (Taberlet et al. 1998). The low temperatures accompanying the Pleistocene glaciations shifted the distribution area of many temperate species southwards (Hewitt 1996). Recent studies show that historical glaciations also affected marine species, with evidence for postglacial range expansions (Wares & Cunningham 2001, Gysels et al. 2004) and multiple refugia along the Atlantic coasts of Western Europe and Great Britain (Coyer et al. 2003, Jolly et al. 2005, Remerie et al. 2006b). Moreover, the sea level drops were responsible for long-term isolation of many marine populations. In the Northwest Atlantic for example, closure of the Strait of Gibraltar isolated populations in the Mediterranean Sea, while NW Europe and the British Isles were largely covered with ice (Dawson 1992). Due to their relatively young age, North European

populations are typically less diverse than their southern counterparts (Hewitt 2000). In view of the limited dispersal in nematodes, we expected to find a clear signature of the Pleistocene glaciations in *R. (P.) marina*.

Several observations indeed indicate that Pleistocene climate changes have affected the population structure of PmII. The mismatch distribution and NCA showed a clear pattern of population expansion, which occurred in two phases: a recent expansion was observed through the English Channel into the North Sea (clade 1-11), and an older expansion along the western and northern coasts of the U.K., into the northern part of the North Sea and the Baltic Sea (Fig. 9.5). Together with the genetic break around the British Isles in all other *R. (P.) marina* species, this suggests that the oldest expansion of PmII occurred before the last Pleistocene glaciation when the landbridge between England and France formed an important barrier for migration into the North Sea (ca. 20 ky BP). The younger expansion then occurred after the formation of the English Channel, some 7.5 ky BP. Similarly, the colonisation of the Baltic Sea postdated 7.5 ky BP and probably consisted of propagules from the oldest expansion event around the British Isles. The distribution of three-level clades highly overlaps in the Southern Bight of the North Sea, which may be indicative of a contact zone between clades from these two expansions. Such a contact zone has also been suggested for the mysid *Neomysis integer* (Remerie et al. 2006b), for the common goby *Pomatoschistus microps* (Gysels et al. 2004), for the brown trout *Salmo trutta* (Garcia-Marin et al. 1999) and for the polychaete *Pectinaria koreni* (Jolly et al. 2005).

A general trend of declining genetic diversity with latitude has been observed in northern temperate species as a result of founder events during expansions (Hewitt 2000, Avise 2000). This pattern was present in *R. (P.) marina*, however, levels of genetic diversity were not significantly lower in the Southern Bight of the North Sea and in Brittany compared to the southern populations. The Southern Bight of the North Sea has intensively been sampled which may confound the diversity estimates in this region. However, haplotype diversity analysed by season was generally high (Derycke et al. 2006) and therefore represents the actual diversity in this area. This high genetic diversity may be explained by a refugial zone around Brittany (Provan et al. 2004) or by a recolonisation from several southern refugia (see Coyer et al. 2003). The distinction between both requires additional sampling in this area. Alternative explanations like massive range shifts through extensive dispersal (Olsen et al. 2004) or slow colonisation with a high proportion of individuals dispersing over small

distances in a continuous front (Nichols & Hewitt, 1994) are unlikely due to the clear signal of range expansion and the limited dispersal of *R. (P.) marina*. Within the Baltic, haplotypic diversity is highest in the Beltic Sea (Fle) and gradually decreases into the western Baltic (Fig 9.6). Pairwise Φ_{st} -values between each of the northern North Sea samples (Sc, No and Sy) and the three Baltic samples (Fle, Ku and Ru) are highest when the western most Baltic sample (Ru) is involved (Appendix 9.1). These patterns correspond with founder events following colonisation from The North Sea and have also been observed in microsatellite data from cod (Nielsen et al. 2003), turbot (Nielsen et al. 2004) and herring (Bekkevold et al. 2005).

Many marine species show distinct genetic breaks between Atlantic and Mediterranean populations, which were isolated from each other due to drastic sea level drops during the last glacial maximum (Remerie et al. 2006a, Sà-Pinto et al. 2005). PmVIII was not encountered in the Atlantic and showed a star shaped pattern suggestive of a recent expansion into the Mediterranean, perhaps from populations along the coasts of West Africa. In contrast, the network of PmV was highly linear and the mismatch distribution showed a multimodal pattern (data not shown). Interestingly, some haplotypes were shared between the Mediterranean, Portuguese and Baltic samples (Fig. 9.3) suggesting that PmV expanded from the Mediterranean after the LGM and colonized the Baltic via occasional long-distance dispersal. In this way, the sympatric distribution of PmII and PmV in the Baltic most likely reflects a recent colonisation rather than a long-term stabile sympatry (Wilke & Pfenninger 2002, Peijnenburg et al. 2004). Its presumed absence in the Atlantic may be the result of competition with species already present in the Atlantic. In this scenario, the populations in the Mediterranean would be relict populations.

MACRO- EVOLUTIONARY PROCESSES AFFECTING RADIATION IN AND DISTRIBUTION OF *R. (P.) MARINA*

The large amount of cryptic species within *R. (P.) marina* raises questions on whether this radiation happened in sympatry or in allopatry. At first sight, the present study corroborates previous findings on the sympatry of several cryptic species of *R. (P.) marina* (Derycke et al. 2005, 2006). This challenges the alleged niche diversification of nonadaptive raditions (Gittenberger 1991), and allopatric speciation as the most commonly observed speciation mechanism in marine species

(Barraclough & Vogler 2000, Wilke & Pfenninger 2002). There are, however, some elements that may point to allopatric speciation in the *R. (P.) marina* complex. First, the global distribution ranges of the species complex indicate that some lineages are highly dominant in particular biogeographic areas: for example PmI dominates the North Sea, while PmVII is restricted to the English Channel and PmVIII to the Mediterranean Sea. Although this might reflect a sampling artefact, this may also indicate adaptation, competition, or monopolisation preventing or reducing the settlement of closely related species. Secondly, at most three species co-occur at a single locality, and nearly all sympatric occurrences are dominated by a single species (Fig. 9.2). Furthermore, the phylogeny based on COI and two nuclear markers showed that PmI and PmIV are sister taxa, just like PmVI-PmIX and PmII-PmX (Fig 9.1). The most closely related species are generally allopatric, and in the few instances where they do co-occur, the abundance of at least one of these most closely related species is always very low (e.g. in Iceland, Roscoff). A similar pattern has been described in other marine species complexes (Suatoni et al. 2006, Mathews 2006) and in the sea urchin genus *Diadema* (Lessios et al. 2001). In view of the similar habitat in which all species were sampled, the distribution of the species complex most likely reflects competitive exclusion between closely related cryptic species (see also Suatoni et al. 2006). Based on the present data, we have no reason to assume that the species show differences in ecological preferences and we therefore find it unlikely that ecological speciation may be at play.

The effects of the Pleistocene glaciations and long-term geographic isolation are believed to have played a key role in the formation of new species (Avice 1994, Hewitt 2000). Estimating the age of an evolutionary event is often dubious, especially when no reliable fossil records are available. The phylogeographic data in PmII indicate that the last glacial maximum had strong impacts on its population genetic structure. Using this biogeographical evidence, COI divergence rates in *R. (P.) marina* range between 21.7 % and 1.3 % divergence per MY. PmII was highly abundant in the northern samples (Norway, North Scotland and the Baltic), suggesting that its range expansion occurred after the last glacial maximum about 14 ky BP (see also Pinceel et al. 2005). This leads to COI mutation rates that are ten times higher than the generally applied molecular clock of 2 % divergence per MY (Knowlton et al. 2000), which might not be that unrealistic given the small body size and short generation time (down to < 5 days, Vranken & Heip 1983) of *R. (P.) marina* which may enhance

mutation rates (Martin & Palumbi 1993). Furthermore, high direct estimates of mitochondrial base substitution mutation rates have been observed in the close relative *Caenorhabditis elegans* (8.9 per site per MY, Denver et al. 2000). An accelerated molecular clock was also proposed for other nematode species, albeit not to the same extent as in our estimate for *R. (P.) marina* (Nieberding et al. 2005, Blouin et al. 1998). The estimated mutation rate of 21.7 % places the speciation events in the *R. (P.) marina* complex in the middle Pleistocene between 210 and 552 ky BP, and consequently predates the last glacial maximum. Likewise, the closure of the Strait of Gibraltar cannot account for the differences between the Mediterranean and Atlantic species. Rather, the restricted gene flow pattern may be suggestive of allopatric speciation occurring irrespective of climate changes.

CONCLUSION

The present study nicely illustrates the extent to which the historical signature of the last glacial maximum is detectable in modern population genetic structure. Pleistocene glaciations and restricted gene flow are undoubtedly highly important micro- evolutionary processes affecting the *R. (P.) marina* species. Our results further indicate that the contemporary distribution of the PmII populations in the Southern Bight of the North Sea is the result of at least two postglacial colonisation events and supports the idea of a contact zone around Brittany/Southern Bight of the North Sea. Our study provides clear evidence for restricted gene flow in all lineages, but at the same time indicates that (effective) long distance dispersal may sporadically occur. We hypothesize that the *R. (P.) marina* species complex has an allopatric origin of speciation, and that the current sympatric distribution is the result of Pleistocene contractions/expansions and occasional random effective long distance dispersal. The present study also proves that meiofauna species living on macroalgae can truly be cosmopolitan, and that this broad-scale distribution is the result of occasional long distance dispersal.

Appendix 9.1: Pairwise Φ_{st} values for the species PmI, PmII, PmIIIa, PmIV, PmV and PmVIII. Sample abbreviations are as in Table 9.1.

PmI	Sc	Ic	Ni	Os	Bl	Ze	Kr	Pa	Br	Sl				
	Sc													
	Ic	0.23309												
	Ni	0.51111	0.56255											
	Os	0.54073	0.59121	0.31607										
	Bl	0.59013	0.61605	0.35484	0.32250									
	Ze	0.43432	0.50314	0.19279	0.16555	0.03143								
	Kr	0.48407	0.54598	0.24705		0.03518	0.13631	0.04279						
	Pa	0.37151	0.45211	0.13455	0.13566	0.07699	0.00047	0.04557						
	Br	0.51747	0.56892	0.26174	0.23815	-0.01090	-0.00039	0.08063	0.03471					
	Sl	0.42231	0.49441	0.16500		0.14991	0.04384	-0.01589	0.03717	0.00061 0.00913				
PmII	No	Sc	Ru	Sy	Fle	Ku	Wa	Pl	Ma	Sa	Sl	Bl	GrB	Pa
	No													
	Sc	0.14034												
	Ru	0.60093	0.50811											
	Sy	0.65591	0.51649	0.71895										
	Fle	0.29255	0.27285	0.45423	0.53760									
	Ku	0.08021	0.16369	0.56206	0.61080	0.27478								
	Wa	-0.01868	0.16918	0.88763	0.69349	0.24990	0.07132							
	Pl	0.16608	0.13270	0.42189	0.43868	0.25761	0.15710	0.14472						
	Ma	0.50769	0.41875	0.59124	0.48577	0.50648	0.46527	0.48883	0.20733					
	Sa	0.29800	0.19673	0.45667	0.33185	0.31381	0.26404	0.29015	0.12426	0.25379				
	Sl	0.81785	0.71510	0.82512	0.72498	0.73240	0.77736	0.82200	0.65785	0.54450	0.60521			
	Bl	0.23429	0.14958	0.34290	0.34745	0.29261	0.18393	0.18265	0.04097	0.06409	0.09250	0.46647		
	GrB	0.25096	0.18126	0.35954	0.31798	0.30121	0.20949	0.19517	0.04460	0.08706	0.10961	0.53043	0.01420	
	Pa	0.41988	0.35548	0.55050	0.47965	0.40529	0.36401	0.39535	0.09634	0.11134	0.20875	0.67009	0.05913	0.01806
PmIII	Va	Bo	NY	Fl	Ze	Pa	Sl	Os	Bl	Ni	GrB			
	Va													
	Bo	0.54604												
	NY	0.32665	0.19372											
	Fl	0.41207	0.17330	-0.00670										
	Ze	0.24120	0.16508	0.03711	0.02401									
	Pa	0.59355	0.27875	0.30626	0.32089	0.14547								
	Sl	0.21022	0.23759	0.06803	0.06418	0.00271	0.17912							
	Os	0.62435	0.21217	0.28024	0.28225	0.10642	0.10928	0.13786						
	Bl	0.41169	0.16019	0.09774	0.08302	-0.00214	0.12351	0.01260	0.01971					
	Ni	0.70309	0.04628	0.10619	0.07369	0.07717	0.28000	0.15811	0.20640	0.08977				
	GrB	0.40058	0.50313	0.34613	0.39971	0.26215	0.48594	0.23717	0.52160	0.37150	0.54264			
PmIV	GrS	Co	San	GrB										
	GrS													
	Co	0.12162												
	San	0.79161	0.91605											
	GrB	0.01688	0.24213	0.86344										
PmV	Sy	He	GrL	Ay	Po									
	Sy													
	He	0.27030												
	GrL	0.43428	0.47821											
	Ay	0.24862	0.24861	0.34461										
	Po	0.24970	0.42042	0.47565	0.41130									
PmVIII	KrB	KrM	GrK	Pal										
	KrB													
	KrM	0.30072												
	GrK	0.32418	0.17087											
	Pal	0.33360	0.18820	0.28349										